Powering Surface Acoustic Wave Device Using Resonant Wireless Power Transfer Techniques

Feixuan Yang
Department of Mathematics, Physics and Electrical Engineering
Northumbria University
Newcastle, United Kingdom
feixuan.yang@northumbria.ac.uk

Haimeng Wu*
Department of Mathematics, Physics and Electrical Engineering
Northumbria University
Newcastle, United Kingdom
haimeng.wu@northumbria.ac.uk

Zhiwei Gao
Department of Mathematics, Physics and Electrical Engineering
Northumbria University
Newcastle, United Kingdom
zhiwei.gao@northumbria.ac.uk

Yongqing Fu (Richard)
Department of Mathematics, Physics and Electrical Engineering
Northumbria University
Newcastle, United Kingdom
richard.fu@northumbria.ac.uk

Jikai Zhang
Department of Mathematics, Physics and Electrical Engineering
Northumbria University
Newcastle, United Kingdom
jikai.zhang@northumbria.ac.uk

Huiling Ong
Department of Mathematics, Physics and Electrical Engineering
Northumbria University
Newcastle, United Kingdom
huiling.ong @northumbria.ac.uk

***Abstract*—This paper investigates the application of resonant wireless power transfer (WPT) technology to surface acoustic wave (SAW) devices. By analyzing the WPT system with SAW devices as loads, this study examines the operating principle of the system and highlights the effect of impedance variation at resonant frequency on power transfer and efficiency. The study also proposes a design to compensate the reactive power generated by the SAW device at resonance. Simulation results show that the proposed asymmetric WPT system designed for SAW devices is 7.4% more efficient than the conventional symmetric compensation topology, and the peak power efficiency of 95.2% using the WPT system to power SAW devices.**

Keywords—wireless power transfer, surface acoustic wave devices, power control system, impedance matching, resonance frequency, charging efficiency.

I. INTRODUCTION

Surface Acoustic Wave (SAW) devices are crucial in various applications due to their unique ability to generate and manipulate acoustic waves on piezoelectric substrates. These devices leverage semiconductor planar processes to create fork-finger-like metal electrodes, known as interdigitated electrodes (IDT), on the substrate surface. When an alternating voltage is applied to these electrodes, they generate surface acoustic waves (SAW) on the substrate's surface [1][2][3].

SAW technology has found widespread applications in emerging fields such as artificial intelligence, autonomous driving, and the Internet of Things (IoT). The high-performance sensors and filters derived from SAW devices are essential for these advanced technologies [5]. Ongoing advancements in manufacturing and testing techniques, as well as research into new materials and structures, continuously improve the performance and cost-effectiveness of SAW devices, further driving their adoption across various industries.

As one example for applications, SAW devices have shown their unique ability to generate acoustic streaming. This remarkable effect enables the creation of controlled currents within liquids or on wet surfaces, effectively disrupting the formation of ice or condensation. By harnessing the power of acoustic waves to rapidly mobilize water molecules, SAW devices can effectively drive the liquid, or prevent the adhesion of ice or the condensation of fog, making them invaluable in various industrial and environmental applications [6].

In certain applications, SAW devices require close proximity to equipment to achieve specific functionalities, such as ice and fog removal from electronic devices or the utilization of acoustic waves to manipulate molecular movement on object surfaces in biological research. These requirements necessitate the miniaturization and portability of SAW devices. However, traditional wired charging methods restrict the practical applications of SAW devices, limiting their portability and flexibility. Moreover, SAW devices demand precise control over their operational parameters, particularly when it comes to the generation and manipulation of acoustic waves. A crucial aspect of this control is the management of energy requirements. High RF power is essential for optimal performance, as it induces localized strong agitation and heating that can enhance the effectiveness of acoustic streaming. However, this increased power demand poses challenges in terms of energy delivery and efficiency. Therefore, alternative power delivery solutions are needed to fully exploit the potential of SAW technology in various fields.

To address these challenges, this paper proposes an innovative solution using a Wireless Power Transfer (WPT) technique to power the SAW devices. WPT

offers unparalleled flexibility and convenience by eliminating the needs for bulky cables and connectors, thus reducing the overall complexity and weight of the system [9][10][11]. This technology is particularly beneficial for powering SAW devices, ensuring they receive the precise amount of energy required for optimal performance.

WPT technology can be broadly classified into near-field and far-field systems. Near-field WPT techniques, such as inductive and capacitive coupling, utilize electromagnetic effects to transmit energy without causing radiation [12]. On the other hand, far-field WPT systems, including microwave radiation and laser-based approaches, radiate electromagnetic energy to enable power transfer over longer distances [13]. One of the key challenges for the WPT systems is the limited efficiency due to their loosely coupled structure [8]. Inductive coupling-based systems, in particular, experience a significant drop in power transfer efficiency as the distance between the transmitter (Tx) and receiver (Rx) coils increases. However, resonant schemes employing coupled resonant coils offer a promising alternative for mid-range WPT applications. By designing the Tx and Rx coils to resonate at the same frequency, high transmission efficiency, longer transmission distances, and increased transmission power can be achieved [14][15][16].

Previous research in wireless charging has predominantly focused on delivering power to loads with a fixed impedance. These fixed impedance loads maintain a consistent electrical resistance and reactance regardless of changes in operating conditions or frequencies [17][18]. Unlike traditional loads, SAW devices exhibit unique characteristics where their impedance varies with the operating frequency, achieving optimal performance precisely at the resonant point. This variation in impedance is due to the piezoelectric properties of the SAW device materials and the design of the IDTs on the substrate. As the operating frequency approaches the resonant frequency, the impedance of the SAW device includes both a real component (resistance) and an imaginary component (reactance), which can change significantly with small shifts in frequency. This impedance variation can result in non-optimal power transfer and efficiency losses if not properly managed. Therefore, the design of a wireless power transfer system for SAW devices must account for these dynamic impedance characteristics to ensure efficient energy delivery and optimal device performance.

Conventional symmetrical WPT compensation techniques, such as series-series (SS) compensation, generate reactive power even at resonance when used to power SAW devices. This issue arises because the equivalent impedance of SAW devices at the resonant frequency includes an imaginary component, distinguishing them from traditional loads. To address this problem, our study proposes an asymmetric compensation topology specifically designed for powering SAW devices. This topology compensates for the imaginary component of the SAW device's impedance at resonance by adjusting the secondary-side capacitance design of the WPT system, thereby eliminating reactive power and maximizing system efficiency. Experimental results demonstrate that the asymmetric WPT compensation topology designed for SAW devices is up to 7.4% more efficient than conventional symmetrical systems, achieving a peak power efficiency of 95.2% when powering SAW devices.

II. Design Methodology

The proposed design aims to efficiently power SAW devices using magnetically resonant WPT. As illustrated in Figure 1, the WPT system consists of a transmitter and a receiver, with the SAW device acting as the load on the receiver side. This asymmetric topology compensates for the imaginary component of the SAW device's impedance at resonance by adjusting the secondary-side capacitance design of the WPT system, thereby eliminating reactive power and maximizing system efficiency. Since the impedance of the SAW device changes with the operating frequency, a variable capacitor can be used in the compensation circuit on the secondary side of the WPT system to adjust the resonance frequency of the WPT supply system as well as the compensation for the imaginary component of the SAW device.

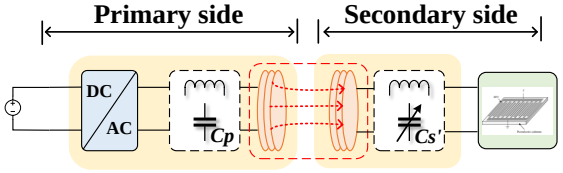

Fig. 1. Powering SAW devices using wireless power transfer.

A. SAW device

The core of this design is the synchronization of the resonant frequencies between the WPT system and the SAW device. By precisely tuning the resonant frequency of the WPT system to match that of the SAW device, we aim to achieve an optimal power transfer efficiency. This approach ensures that the WPT system and the SAW device are operated at the same frequency, maximizing the coupling between the transmitter and receiver coils and also minimizing power losses.

To accomplish this, we firstly analyze the resonant characteristics of the SAW device. The resonant frequency of a SAW device is determined by its physical dimensions and material properties [3].

$$\begin{cases} \lambda = 4d \\ f_0 = \frac{v}{\lambda} \end{cases} \quad (1)$$

where, λ is SAW wavelength, d is electrode width in SAW, f_0 is the resonant frequency of SAW, and v is SAW's wave velocity.

In this paper, an electrical equivalent circuit model is used to describe the resonant behavior of the SAW resonator. A conceptual diagram of the SAW

resonator is shown in Figure 2(a) [4]. The corresponding electrical equivalent circuit at the resonance frequency is shown in figure 2(b), where C_0 is the static capacitance which represents the fixed dielectric capacitance of the resonator, L_m and C_m are the motional inductance and capacitance, which are corresponding to the contribution of inertia and elasticity, respectively, and R_m is the motional resistance which is corresponding to the contribution of damping [19]. These parameters can be calculated from the resonance frequency f_r, anti-resonance frequency f_{ar}, conductance G and quality factor Q_r at resonance frequency of the SAW resonator. The equations for the calculation of these parameters are given as

$$R_m = G_r^{-1} \tag{2}$$

$$C_m = \frac{1}{\omega_r Q_r G_r} \tag{3}$$

$$C_0 = \frac{C_m}{(\omega_{ar} - \omega_r)^2 - 1} \tag{4}$$

$$L_m = \frac{Q_r G_r}{\omega_r} \tag{5}$$

where G_r is the peak value of the conductance, $\omega_r = 2\pi f$ is the angular frequency of the SAW resonator, and $\omega_{ar} = 2\pi f_{ar}$ is the angular frequency at anti-resonance.

The quality factor Q_r at resonance of SAW resonator is determined as [19]

$$Q_r = \frac{f_r}{\Delta f} \tag{6}$$

where Δf is the bandwidth at half of the peak conductance.

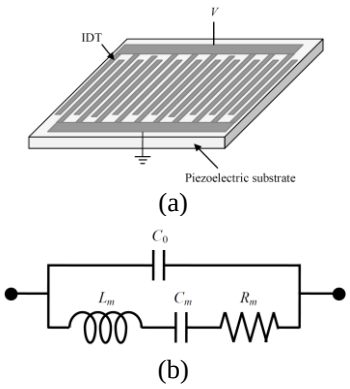

Fig. 2. (a) Schematic of a one port SAW resonator with large number of IDT electrodes without reflectors and (b) electrical equivalent circuit of a one port SAW resonator.

The equivalent impedance of the SAW can be obtained from:

$$Z_{SAW} = \frac{1}{\dfrac{1}{R_m + j(\omega L_m - \dfrac{1}{\omega C_m})} + j\omega C_0} \tag{7}$$

When in the resonant state, the equivalent impedance of the SAW device can be written as:

$$Z_r = \frac{1}{\dfrac{1}{R_m} + j\omega C_0} \tag{8}$$

Based on the application of SAW devices for agitation for defogging or drug delivery, we chose a frequency of 13.5 MHz SAW devices as an example for our study. As shown in Fig. 3, the impedance of the 13.5 MHz SAW device at various frequencies can be determined by applying the relevant parameters of the SAW device into the formula. It is observed that both the real and imaginary components of the SAW device's impedance are minimal at the resonant frequency, while the impedance increases significantly at the anti-resonance point. Therefore, ensuring frequency matching is crucial in the design of WPT systems to optimize performance and efficiency.

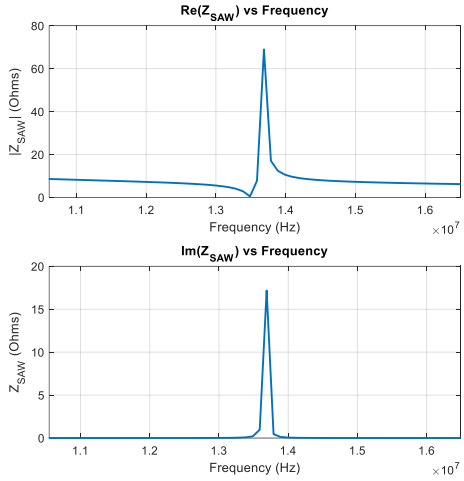

Fig. 3. The impedance of the 13.5MHz SAW device at different frequencies.

Figure 4 shows the impedance of the selected 13.5 MHz SAW device at the resonant frequency using a network analyzer. The measurements confirm that at the resonant frequency of 13.5 MHz, the SAW device still exhibits an imaginary component in its impedance. To address this, an optimized WPT compensation topology is required to compensate for this imaginary component, thereby maximizing efficiency.

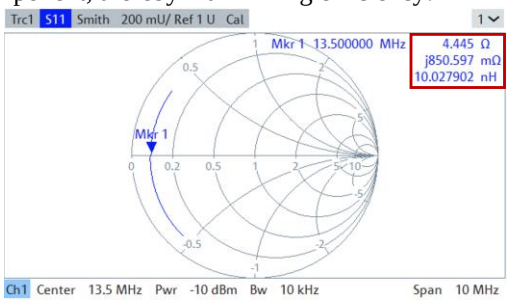

Fig. 4. Impedance of SAW device at resonant frequency 13.5MHz.

B. Wireless Power Transfer System

The WPT system is designed with a resonant circuit that matches the resonant frequency of the SAW device. This circuit typically consists of inductive elements, such as coils, and capacitive elements that are tuned to resonate at the desired frequency.

When we choose the typical SS compensation topology in WPT as shown in Fig. 5, we can obtain the following equations:

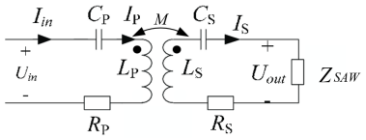

Fig. 5. SS compensation equivalent circuit

$$\begin{cases} [R_p + j(\omega L_p - \frac{1}{\omega C_p})]I_p - j\omega M I_s = U_{in} \\ j\omega M I_p - [R_s + Z_{SAW} + j(\omega L_s - \frac{1}{\omega C_s})]I_s = 0 \end{cases} \quad (9)$$

where, U_{in} is input voltage, I_p and I_s are the currents flowing through the transmitting and receiving coils respectively, and ω is the angular frequency of U_{in}. Therefore, we can obtain:

$$I_p = \frac{U_{in}}{Z_p + \frac{\omega^2 M^2}{Z_s}} \quad (10)$$

$$I_s = -\frac{j\omega M Y_s U_{in}}{Z_p + \frac{\omega^2 M^2}{Z_s}} \quad (11)$$

where, $Z_p = R_p + j(\omega L_p - \frac{1}{\omega C_p})$, $Z_s = R_s + Z_{SAW} + j(\omega L_s - \frac{1}{\omega C_s})$, Y_s is the reciprocal of Z_s.

In a conventional symmetrical compensation topology, the inductance and capacitance are designed to satisfy the following conditions:

$$\begin{cases} \omega L_p - \frac{1}{\omega C_p} = 0 \\ \omega L_s - \frac{1}{\omega C_s} = 0 \end{cases} \quad (12)$$

At this point, the primary and secondary side capacitors are designed as follows:

$$\begin{cases} C_p = \frac{1}{\omega^2 L_p} \\ C_s = \frac{1}{\omega^2 L_s} \end{cases} \quad (13)$$

According to this design approach, when the resonant frequencies are matched, the impedance of both the primary and secondary sides of the WPT system can be expressed as follows:

$$\begin{cases} Z_p = R_p \\ Z_s = R_s + \frac{1}{\frac{1}{R_m} + j\omega C_0} \end{cases} \quad (14)$$

It can be observed that the secondary impedance contains an imaginary component generated by the SAW device in the resonant state. To maximize active power transfer, it is necessary to design suitable capacitors such that the equivalent impedances on both the primary and secondary sides are purely real. In other words, $Z_p$and Z_s should be purely real.

Therefore, the design conditions are:

$$\begin{cases} \omega L_p - \frac{1}{\omega C_p} = 0 \\ Im(Z_{SAW}) + j\left(\omega L_s - \frac{1}{\omega C_s'}\right) = 0 \end{cases} \quad (15)$$

As a result, the capacitance designed to compensate for the imaginary component of the secondary SAW device at resonance is given by:

$$\begin{cases} C_p = \frac{1}{\omega^2 L_p} \\ C_s' = \frac{1}{\omega(\omega L_s + Im(Z_{SAW}))} \end{cases} \quad (16)$$

In the design of this WPT system, we use coils with: $L_p = L_s = 4.2\ \boldsymbol{\mu}H$, $C_p = 37\ pF$, $C'_s = 33\ pF$.

Since both the equivalent input impedance Z_p and the secondary side equivalent impedance Z_s of the system are purely resistive, the input power of the wireless energy transmission system is expressed as:

$$P_{in} = U_{in} I_p = \frac{(R_s + R_{SAW}){U_{in}}^2}{R_p(R_s + R_{SAW}) + \omega^2 M^2} \quad (17)$$

The output power is:

$$P_{out} = {I_s}^2 R_{SAW} = \frac{\omega^2 M^2 {U_{in}}^2 R_{SAW}}{[R_p(R_s + R_{SAW}) + \omega^2 M^2]^2} \quad (18)$$

The transmission efficiency is obtained from:

$$\eta = \frac{P_{out}}{P_{in}} = \frac{\omega^2 M^2 R_{SAW}}{(R_s + R_{SAW})[R_p(R_s + R_{SAW}) + \omega^2 M^2]} \quad (19)$$

Using the above formulas, the relationship between efficiency and mutual inductance for different compensation methods was determined, as shown in Fig. 6. It was observed that the proposed asymmetric compensation system exhibits higher efficiency compared to the traditional symmetric compensation topology. Furthermore, this efficiency difference becomes more pronounced as the mutual inductance increases. This indicates that the asymmetric compensation method is more effective in maximizing power transfer efficiency, particularly at higher levels of mutual inductance.

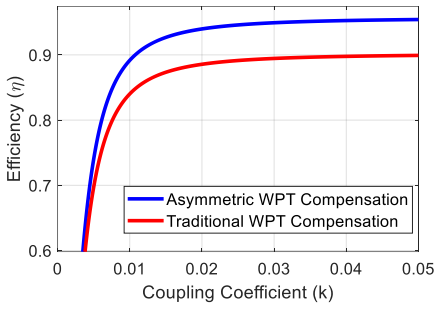

Fig. 6. Efficiency vs coupling coefficient for different compensation methods.

C. Control system

In this study, the proportional–integral (PI) control strategy is used to control the operating power of the SAW device, as shown in Fig. 7. For power control of SAW devices, the PI controller controls the output power by adjusting the duty cycle of the inverter switches to affect the output voltage and current. The goal is to modulate the operating performance of the SAW device such as the surface temperature or the

speed of the drug delivered as a patch by controlling the power of the SAW device.

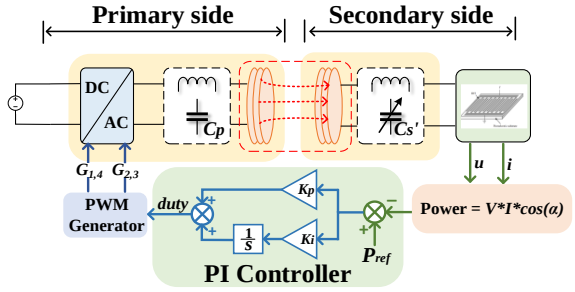

Fig. 7. Schematic of wireless powered SAW device with power controller.

III. Simulation & Experiment Results

A. Analysis of 13.5MHz WPT

During the simulation, we utilized a 13.5 MHz WPT system to determine the coupling coefficients at various distances and assess the efficiency of the WPT system. The simulation results were subsequently compared and verified through experiments, as detailed in Table I. The discrepancy between the simulated and experimental efficiencies of the WPT system was found to be approximately 5% at most. This small margin of error suggests that the simulation closely mirrors the real-world performance of the power supply system. Consequently, we will proceed with further simulations to validate our findings comprehensively.

TABLE I. Results of Experiment of 13.5MHz WPT System

Distance (cm)	*Coupling coefficient*	*Efficiency in experiment*	*Efficiency in simulation*
1.5	0.1519	77.09%	77.79%
2	0.0826	49.77%	54.57%
2.5	0.0721	43.59%	48.35%

During the experiment, we used the 13.5MHz WPT system and varied the distances between the two coils, and investigate the relationship between distance, coupling coefficient and efficiency as shown in Fig. 8.

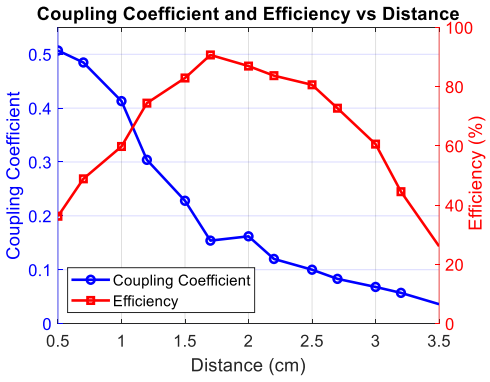

Fig. 8. Coupling coefficient and efficiency of WPT system at different distances.

B. 13.5MHz SAW Powered by WPT System

In this simulation, our study verifies the optimal design of the WPT system for SAW devices. The specific device parameters used for the simulation are shown in Table II.By improving the value of the secondary capacitor designed to compensate for the reactive power generated by the SAW device at the coupling frequency, we have enhanced the power transfer efficiency by up to 7.4%.

Additionally, we performed a comparative analysis to investigate the transmission efficiency over different coupling coefficients. This analysis compares the efficiency of traditional symmetrical WPT compensation with the proposed asymmetric WPT compensation. The results of this comparison are shown in Fig. 9. The experimental results confirm that our proposed design achieves higher efficiency, particularly at higher coupling coefficients. Moreover, the simulation results align with our theoretical analysis, further validating the effectiveness of our design in optimizing the system's performance. Furthermore, Fig. 10 illustrates the current and voltage across the transmitting coil, as well as the current and voltage across the SAW device during operation.

TABLE II. The Design Parameters of the System

U_{in}	20 V
Switching frequency	13.5 MHz
L_p, L_s	4.2 uH
C_p	37 pF
C'_s	33 pF

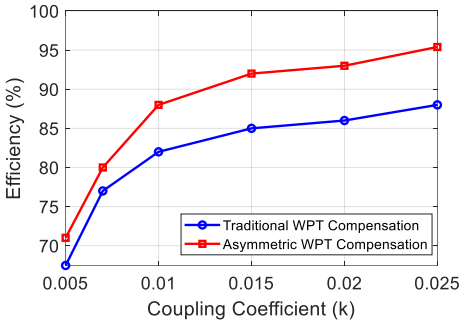

Fig. 9. Efficiency Comparison of Traditional and Asymmetric WPT Compensation.

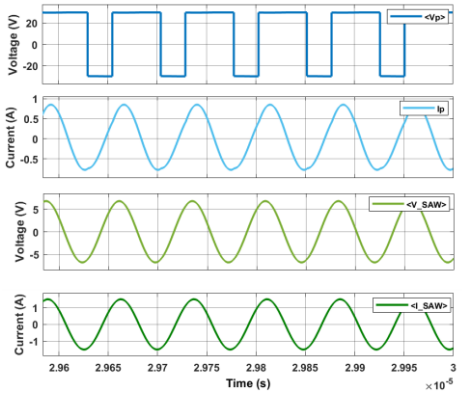

Fig. 10. Voltage and current into the transmitter coil and SAW device.

C. *Power Control for WPT system Powering SAW Devices*

When using SAW devices for de-icing, defogging, or as drug delivery patches, the power level significantly impacts the temperature and operational efficiency of the SAW devices. To ensure optimal performance across various applications, we implemented a PI closed-loop control system to regulate the power. The PI control system adjusts the power output based on real-time feedback, maintaining the SAW devices in a stable and efficient operating state.

Fig. 11 shows the WPT system with power control functionality constructed in the simulation. To test the response and stability of this control system, we changed the set power value at 20 us during the simulation. This test allows us to observe how the system adjusts the output power to meet the new setpoint and evaluate the dynamic performance and regulation capability of the PI control under varying power demands. The simulation results confirm the effectiveness and reliability of the PI closed-loop control in maintaining efficient operation of SAW devices under different power conditions. The experimental results are shown in Fig. 12.

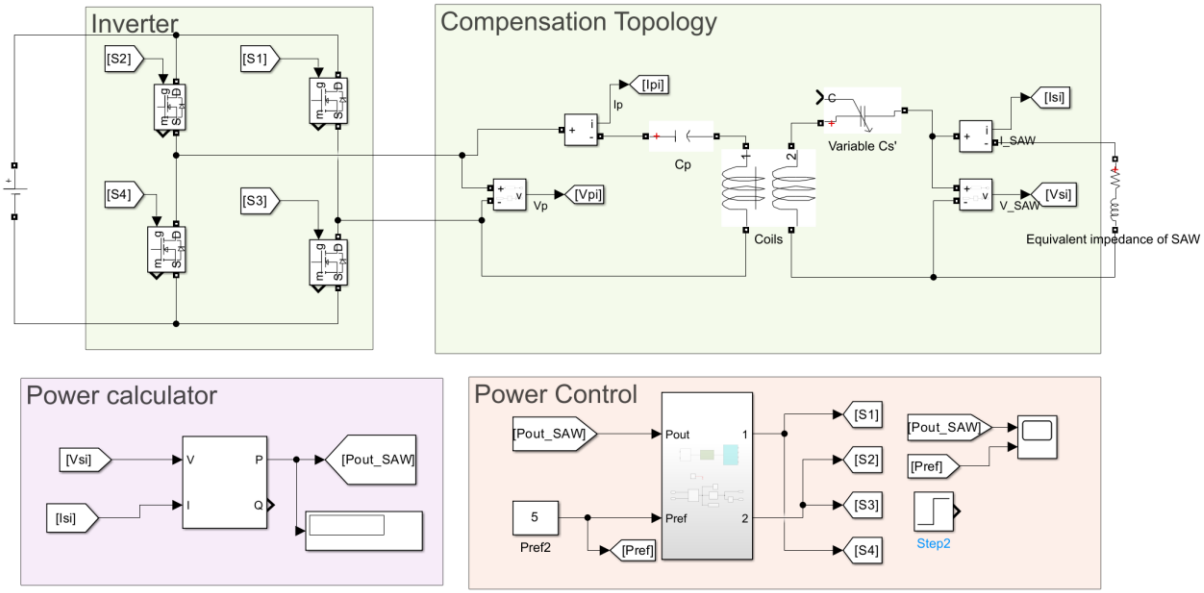

Fig. 11. Power Control system for WPT system with SAW Load.

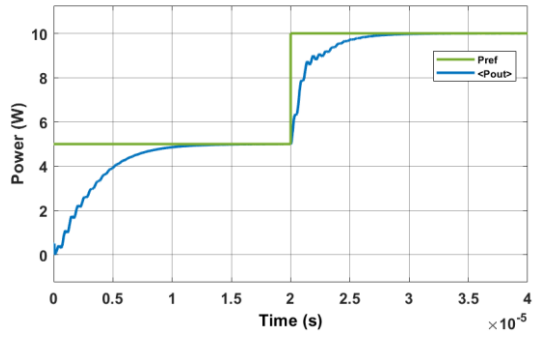

Fig. 12. Simulation results for power control when Pref is changed from 5W to 10W.

IV. Conclusion

This paper proposes an asymmetrical SS compensation topology specifically for powering SAW devices, which compensates for the imaginary component of the SAW device's impedance at the resonance frequency, aiming to eliminate reactive power and maximize system efficiency. A detailed analysis of the impedance characteristics of SAW devices is carried out, along with the design of an optimized WPT system tailored to these characteristics. Experimental and simulation results indicate that the proposed WPT system achieves optimal performance when the resonant frequency is matched with that of the SAW device. The experimental results demonstrate that the asymmetric WPT system designed for the SAW devices is up to 7.4% more efficient than those traditional symmetrical WPT compensation techniques, achieving a peak power efficiency of 95.2% when powering SAW devices.

V. Reference

[1] D. P. Morgan, "A history of surface acoustic wave devices," Int. J. High Speed Electron. Syst., vol. 10, no. 3, pp. 553-602, 2000, doi: 10.1142/S0129156400000593.

[2] M. B. Mazalan, A. M. Noor, Y. Wahab, S. Yahud, and W. S. W. K. Zaman, "Current development in interdigital transducer (IDT) surface acoustic wave devices for live cell in vitro studies: A review," Micromachines, vol. 13, no. 1, p. 30, 2022, doi: 10.3390/mi13010030.

[3] Y. Q. Fu, J. K. Luo, X. T. Du, A. J. Flewitt, Y. Li, G. H. Markx, A. J. Walton, and W. I. Milne, "Recent developments on ZnO films for acoustic wave based bio-sensing and microfluidic applications: A review," Sens. Actuators B Chem.

[4] A. K. Namdeo and H. B. Nemade, "Simulation on effects of electrical loading due to interdigital transducers in surface

acoustic wave resonator," Procedia Eng., vol. 64, pp. 322-330, 2013.

[5] S. Zhang et al., "Surface acoustic wave devices using lithium niobate on silicon carbide," IEEE Trans. Microw. Theory Tech., vol. 68, no. 9, pp. 3653-3666, Sept. 2020, doi: 10.1109/TMTT.2020.3006294.

[6] A. Grossi, K. Yadav, and M. A. Lawson, "Mechanical stimulation increases proliferation, differentiation and protein expression in culture: Stimulation effects are substrate dependent," J. Biomech., vol. 40, pp. 3354-3362, 2007.

[7] Y. Q. Fu, J. K. Luo, N. T. Nguyen, A. J. Walton, A. J. Flewitt, X. T. Zu, Y. Li, G. McHale, A. Matthews, E. Iborra, H. Du, and W. I. Milne, "Advances in piezoelectric thin films for acoustic biosensors, acoustofluidics and lab-on-chip applications,".

[8] H. Wu, X. Wang, B. Gu, and V. Pickert, "Investigation of a GaN-based bidirectional wireless power converter using resonant inductive coupling," in Proc. IEEE Wireless Power Transf. Conf. (WPTC), 2019, pp. 263-268.

[9] S. Li and C. C. Mi, "Wireless power transfer for electric vehicle applications," IEEE Trans. Emerg. Sel. Topics Power Electron., vol. 3, no. 1, pp. 4-17, Mar. 2015.

[10] M. Fu, T. Zhang, P. C.-K. Luk, X. Zhu, and C. Ma, "Compensation of cross coupling in multiple-receiver wireless power transfer systems," IEEE Trans. Ind. Inform., vol. 12, no. 2, pp. 474-482, Apr. 2016.

[11] Z. Pantic, K. Lee, and S. M. Lukic, "Receivers for multifrequency wireless power transfer: Design for minimum interference," IEEE Trans. Emerg. Sel. Topics Power Electron., vol. 3, no. 1, pp. 234-241, Mar. 2015.

[12] H. Wu, B. Gu, X. Wang, V. Pickert, and B. Ji, "Design and control of a bidirectional wireless charging system using GaN devices," in Proc. IEEE Appl. Power Electron. Conf. Expo. (APEC), 2019, pp. 864-869.

[13] A. A. Eteng, S. K. A. Rahim, C. Y. Leow, S. Jayaprakasam, and B. W. Chew, "Low-power near-field magnetic wireless energy transfer links: A review of architectures and design approaches," Renew. Sustain. Energy Rev., vol. 77, pp. 486-505, Sep. 2017.

[14] K. Detka and K. Górecki, "Wireless power transfer—A review," Energies, vol. 15, p. 7236, 2022, doi: 10.3390/en15197236.

[15] X. Mou, D. T. Gladwin, R. Zhao, and H. Sun, "Survey on magnetic resonant coupling wireless power transfer technology for electric vehicle charging," IET Power Electron., vol. 12, pp. 3005-3020, 2019, doi: 10.1049/iet-pel.2019.0529.

[16] M. A. Yousuf, T. K. Das, M. E. Khallil, N. A. A. Aziz, M. J. Rana, and S. Hossain, "Comparison study of inductive coupling and magnetic resonant coupling method for wireless power transmission of electric vehicles," in Proc. 2021 Int. Conf. Robot. Electr. Signal Process. Techn. (ICREST), Dhaka, Bangladesh, Jan. 2021, pp. 737-741.

[17] H. Li, J. Xu, F. Gao, Y. Zhang, X. Yang, and H. Tang, "Duty cycle control strategy for dual-side LCC resonant converter in wireless power transfer systems," IEEE Trans. Transp. Electrif., vol. 8, no. 2, pp. 1944-1955, June 2022, doi: 10.1109/TTE.2021.3123340.

[18] W. Zhang and C. C. Mi, "Compensation topologies of high-power wireless power transfer systems," IEEE Trans. Veh. Technol., vol. 65, no. 6, pp. 4768-4778, June 2016, doi: 10.1109/TVT.2015.2454292.

[19] K.-Y. Hashimoto, Surface Acoustic Wave Devices in Telecommunications: Modelling and Simulation. New York: Springer-Verlag, 2000.